Plant Physiology and Biochemistry 223 (2025) 109899

Contents lists available at ScienceDirect

Plant Physiology and Biochemistry

journal homepage: www.elsevier.com/locate/plaphy

Microstructural characterization of cacao seeds during controlled transformation through microscopy techniques and image analysis: Insights into quality-related attributes

Lili Dahiana Becerra [a], María Ximena Quintanilla-Carvajal [a], Jorge Martínez Herrera [b], María de Jesús Perea-Flores [c], Sebastián Escobar [d,e], Ruth Yolanda Ruiz [a,*]

[a] Grupo de Investigación en Procesos Agroindustriales, Facultad de Ingeniería, Universidad de La Sabana, Campus Universitario del Puente del Común, Km 7 Autopista Norte de Bogotá, Chía, Cundinamarca, Colombia
[b] Universidad Politécnica de Huatusco, Predio Axol S/N, Reserva Territorial, C.P. 94106, Huatusco de Chicuellar, Veracruz, Mexico
[c] Centro de Nanociencias y Micro y Nanotecnologías, Instituto Politécnico Nacional (IPN), Av. Luis Enrique Erro S/N, Unidad Profesional Adolfo López Mateos, Zacatenco, Gustavo A. Madero, C.P. 07738, Ciudad de México, Mexico
[d] Process & Quality Cacao Laboratory, Centro de Investigación Palmira, Corporación Colombiana de Investigación Agropecuaria (Agrosavia), Palmira, Valle del Cauca, Colombia
[e] Cacao of Excellence Programme, Bioversity International, Italy

ARTICLE INFO

Keywords:
Controlled cacao postharvest transformation
Organic acids
Anthocyanins
Autofluorescence
Microstructure

ABSTRACT

The controlled transformation of cacao seeds by adjusting the pH by using organic acid solutions is valuable for obtaining high-quality products with enhanced characteristics. This study aimed to evaluate the impact of organic acids on the microstructure of cacao seeds under specific operating conditions that emphasize cacao quality-related characteristics. Confocal laser scanning microscopy and scanning electron microscopy were employed to describe the seed microstructure and characterize the presence of autofluorescent cellular components through image analysis, as well as to obtain the fractal dimension and texture parameters of the seeds. The results revealed significant differences in the microstructural characteristics of the seeds among the different treatments applied. Acetic acid treatment increased membrane permeability, causing a reduction in cell volume. In contrast, lactic acid treatment resulted in the formation of smaller vacuolar inclusions of anthocyanins within the cotyledon, accompanied by a higher presence of phenolic compound aggregates. Conversely, the controlled transformation using citric acid resulted in minimal cell damage to the seed structures, resulting in a more uniform and homogeneous texture. These findings provide valuable insights into the microstructural changes induced by organic acids and their potential to improve cacao processing methods, focusing on enhancing quality-related aspects vital for developing cacao products.

1. Introduction

Cacao seeds are the primary raw material for chocolate production and undergo multiple processing stages to achieve the desired commercial quality. Beyond their distinct flavor, cacao seeds have a complex microstructure intricately linked to their diverse and dynamic chemical composition, which plays a key role in determining their quality and sensory characteristics. Understanding the microstructural changes that occur during postharvest processing is essential for gaining insights into the underlying mechanisms and transformations involved. This knowledge could lead to the optimization of postharvest processes, ultimately contributing to improved cacao quality (Elwers and Lieberei, 2020).

Postharvest treatments of cacao seeds, primarily fermentation and drying, are essential in developing the desired flavor and quality of chocolates. Spontaneous fermentation (SF), driven by microbial activity, initiates biochemical reactions within the seeds and generates heat, leading to a natural increase in temperature. This process promotes the formation of complex flavor precursors, contributing to the characteristic chocolate attributes. In contrast, controlled transformation, an alternative to SF, involves the diffusion of organic acids into the seeds, regulating the seeds environment to maintain a specific temperature and pH level (Becerra et al., 2022; John et al., 2016). This method allows for

* Corresponding author.
E-mail address: ruth.ruiz@unisabana.edu.co (R.Y. Ruiz).

https://doi.org/10.1016/j.plaphy.2025.109899
Received 17 January 2025; Received in revised form 4 March 2025; Accepted 6 April 2025
Available online 7 April 2025

precise control over the biochemical changes occurring within the seeds, influencing their chemical composition and quality. Both fermentation and controlled transformation induce various chemical reactions that alter the seeds' endogenous components, leading to modifications at both macro and microstructural levels. These changes significantly impact the flavor profile, texture, and overall quality of the cacao, making it essential to understand these processes for optimizing post-harvest methods.

Although research on the microstructural changes of cacao seeds is still advancing, existing studies have revealed several significant phenomena that could influence the quality of chocolates (Andersson et al., 2006; Biehl et al., 1982; Brillouet and Hue, 2017). Notably, the breakdown of vacuoles containing phenolic compounds (Barišić et al., 2019), which can affect the astringency and bitterness of cacao, is one such key change. The degradation of protein bodies, critical for texture and mouthfeel, is another observed change, impacting the solubility and functionality of proteins during chocolate production. Additionally, the agglomeration of lipid bodies and cellular disruption play a role in altering the texture and flavor of chocolate. These microstructural changes have been characterized using microscopic techniques, including transmission electron microscopy (TEM), scanning electron microscopy (SEM), and confocal laser scanning microscopy (CLSM) (Andersson et al., 2006; Biehl et al., 1982; de Brito et al., 2001; Elwers et al., 2010; Martini et al., 2008).

Confocal laser scanning microscopy (CLSM) and scanning electron microscopy (SEM) have emerged as powerful tools for investigating microstructural changes in foods and materials (Aguilera, 2005, 2022). These advanced techniques enable the visualization and characterization of cellular structures and their components. CLSM, for example, allows the evaluation of fluorescence intensity and patterns of chemical components in food, providing insights into composition, structure, and compound localization within the food matrix (Auty, 2013). On the other hand, SEM provides detailed information on the structure, morphology, and texture (Stokes, 2013). The application of these techniques has evolved from qualitative, observer-dependent descriptions to obtaining quantitative and detailed insights into morpho-colorimetric food features through image analysis and processing (Hernández-Carrión et al., 2015). Additionally, these findings can be correlated with relevant physical and chemical data obtained from other analytical methods, facilitating a deeper understanding of micrometric-level changes.

This study aims to evaluate the effect of controlled transformation on the microstructure of cacao seeds, with spontaneous fermentation as a reference process, to provide critical insights into how microstructural changes influence key quality attributes, and to enhance the understanding of the mechanisms underlying cacao transformation. Advanced microscopy techniques, including CLSM, SEM, and image analysis, were employed to quantitatively assess the microstructural changes induced by controlled transformation. Additionally, the study explores the impact of these processes on the chemical composition of the seeds, focusing on total tannin content, total phenolic content, and antioxidant activity. These compounds are particularly relevant as they are associated with three key factors critical to cacao quality: the color of the matrices, where polyphenols and tannins contribute to the development of desirable red-pink hues; the sensory profile, with these compounds influencing key flavor attributes such as bitterness, astringency, and overall taste; and the content of bioactive compounds, where antioxidant activity serves as an important indicator of the nutritional and health-related value of the cacao seeds. The findings complement previous studies, providing a first step toward understanding how controlled transformation-induced microstructural changes drive the physicochemical alterations that influence these key quality parameters.

2. Material and methods

2.1. Cacao material

Fresh and healthy cacao pods of Theobroma Corpoica La Suiza clone (TCS01) were purchased from the Boyacá Department in Colombia. The pods were carefully chosen to ensure they were free from visible defects and diseases, ensuring the integrity of the cacao material for subsequent processing and analysis.

2.2. Cacao postharvest operations

2.2.1. Spontaneous fermentation (SF)

The pods of the TCS01 cultivar were opened immediately after harvesting, and the seeds were placed in a wooden fermenter. The initial aeration of the cacao mass occurred manually after 48 h, during which the mass of seeds was mixed to ensure uniform fermentation. This aeration process was repeated every 24 h until a total fermentation of 144 h was achieved. Sampling for evaluation of key quality attributes was performed every 24 h, with each sample consisting of 10 seeds. For CLSM and chemical characterization, the samples were frozen at −80 °C until further analysis. Samples designated for SEM analysis were immediately fixed, as detailed in section 2.4.3.

2.2.2. Controlled transformation of cacao seeds (CT)

Cacao seeds were subjected to controlled transformation with organic acids (OA) under three distinct experimental conditions, each designed to evaluate specific attributes related to quality and market value. These conditions were selected based on previous research findings and aimed to achieve: i) an outstanding sensory profile in chocolate (Trial AA) (Becerra et al., 2024), ii) increased levels of bioactive compounds in cacao beans (Trial LA), and iii) the development of red-pink hues in the cacao beans (Trial CA) (Becerra et al., 2023). The experimental conditions for each trial are detailed in Table 1.

The controlled transformation of cacao seeds was conducted following the methodology outlined by Becerra et al. (2022). Briefly, 180 g of cacao seeds were placed into 500 mL conical flasks containing 300 mL of organic acid solution at the concentrations specified in Table 1. The conical flasks were then placed in incubator shakers with a constant stirring rate of 100 rpm and temperature controlled according to the conditions listed in Table 1. The cacao seeds were sampled at 24, 48, and 72 h of controlled transformation. Samples designated for CLSM and chemical characterization were immediately frozen at −80 °C to maintain their microstructural integrity and chemical composition until analysis. Samples for SEM were immediately subjected to the fixation process, as described in section 2.4.3.

2.3. Chemical characterization of transformed cacao beans

2.3.1. Sample preparation

The transformed cacao seeds (SF, CT) were washed and then subjected to a controlled drying process in a forced convection drying oven (Memmert UF 110, Schwabach, Germany) at 50 °C for 48 h to obtain dried cacao beans. Subsequently, the dried beans were deshelled and ground using a coffee grinder (KitchenAid, Benton Harbor, MI, USA). The ground cacao samples were defatted with *n*-hexane in an ultrasonic bath for 20 min. This defatting procedure was performed twice to ensure the complete removal of lipids, yielding ground, and defatted cacao

Table 1
Experimental conditions for cacao seeds transformation.

Trial	Organic Acid (OA)	Temperature (°C)	OA Concentration (g/L)
AA	acetic acid	30	1
LA	lactic acid	45	1
CA	citric acid	45	30

beans. Polyphenolic compounds were extracted according to the method described by Becerra et al. (2023). In summary, 75 mg of ground and defatted cacao beans underwent ultrasound-assisted extraction using 3 mL of an 80:20 (v/v) methanol-water solution for 15 min. The extract was then vortexed for 3 min and centrifuged at 6000 rpm (4400 rcf) at 4 °C for 10 min. This process was repeated twice more. The combined supernatants were evaporated to dryness, and the resulting concentrate was reconstituted in 3 % acetonitrile and filtered through a 0.22 μm PVDF membrane.

2.3.2. Determination of total polyphenol content (TPC)

The total phenolic content (TPC) of extracts was determined according to the method proposed by Singleton and Rossi (1965), with some modifications and adaptation to a 96-well microplate. An aliquot (50 μL) of the sample extract was mixed with 100 μL of Folin-Ciocalteu aqueous reagent (10 % v/v). After 3 min, 100 μL of a 7.5 % Na_2CO_3 solution was added. After standing for 2 h in the dark, absorbance was measured at 755 nm. All determinations were performed in triplicate. A calibration curve with increasing gallic acid concentrations was used to compute TPC values. The results were expressed as mg of gallic acid equivalents (GAE) per g of cacao.

2.3.3. Determination of total tannin content (TTC)

The total tannin content (TTC) was measured using a colorimetric method outlined by Barbosa-Pereira et al. (2018). In summary, 25 μL of the sample extract was mixed with 250 μL of a 4 % vanillin reagent solution in methanol/hydrochloric acid 37 % (2:1 v/v) in a 96-well microplate. This mixture was incubated at 25 °C for 20 min, and the absorbance was measured at 500 nm. Each sample was tested in triplicate. A calibration curve was created using a catechin standard solution. The tannin content was reported as mg of catechin equivalents (CE) per g of cacao.

2.3.4. Antioxidant activity assays

The antioxidant activity of extracts was measured by ABTS (2,2′-azino-bis-(3-thylbenzothiazolne-6-sulfonic acid) diammonium salt) (Re et al., 1999) and DPPH (2,2-diphenyl-1-picrylhydrazyl radical) (Brand-Williams et al., 1995) methods. The absorbance was measured at 734 nm and 515 nm, respectively. All samples were analyzed in triplicate. The results were obtained from a calibration curve using Trolox in both cases. Results were expressed in mg Trolox equivalent per g of cacao.

2.4. Microstructural characterization of cacao seeds

2.4.1. Confocal laser scanning microscopy (CLSM)

Prior to sectioning, the frozen seeds were gradually thawed at 4 °C. The seeds were then cut into slices approximately 0.5 cm thick using a blade. Each sample was then mounted on glass slides and observed under a confocal laser scanning microscope (Olympus, FV 1000, Japan) using a 20X/0.8 objective lens. Laser wavelengths used for excitation were 405 nm, 559 nm, and 635 nm. The autofluorescence was detected and the RGB images were saved in TIFF format with a 976 x 976 pixels resolution.

2.4.2. Image analysis

The images obtained through CLSM with an excitation laser at 559 nm were analyzed using ImageJ software version 1.53e (Bethesda, Maryland, USA) (Schneider et al., 2012). The autofluorescence associated with polyphenolic compounds (red color) was quantified by extracting the a^* color coordinate from the CIELab color space for each treatment, using the "Color Space Converter" plugin.

For particle analysis associated with accumulation of polyphenolic compounds, the images were initially enhanced by adjusting the contrast by 0.5 %. The images were then converted to a binary format by applying a threshold range of 40–94, where pixels within this range were turned black, and those outside it were turned white. Subsequently, the "Analyze Particles" routine was applied to the processed images. This analysis provided three key metrics: the number of particles, their size, and their area.

2.4.3. Scanning electron microscopy (SEM)

Cacao seeds were divided into longitudinal and transverse sections of approximately 0.5 cm thickness using a blade. The samples were fixed in 4 % glutaraldehyde (v/v) and 2 % paraformaldehyde (v/v) in 0.2 M phosphate buffer, pH 7.2, for 72 h. Subsequently, the fixed tissues were dehydrated through an ascending ethanol series: 30 %, 40 %, 50 %, 60 %, 70 %, 80 %, 90 %, and 95 % (v/v) for 2 h each, and twice in 100 % ethanol for 2 h. Subsequently, the sections were subjected to critical point drying with CO_2 using Samdri-795 equipment (Tousimis, MD, USA). The dried samples were immobilized on glass slides using double-sided carbon adhesive tape and coated with gold for 70 s using a sputter coater (Denton Vacuum, NJ, USA) to enhance electron conduction into the material. Finally, the samples were placed into the Scanning Electron Microscope chamber (JSM-6490 LV, Jeol, California, USA) at an acceleration voltage of 6 kV and a working distance of 10 mm. Images were acquired in 500x, 1000x, and 5000× magnifications, and stored in TIFF format at 1536× 858 pixels.

2.4.4. Texture image analysis

The image processing was performed according to Hernández-Carrión et al. (2015). The images acquired through SEM were stored as grayscale bitmaps with brightness values ranging from 0 to 255 for each pixel in the image. The fractal dimension of the images (FDt) was evaluated using the method of changing differential box-counting (Chen et al., 2001) with ImageJ software version 1.53e. The SEM images at 500× magnification were analyzed, considering both longitudinal and transverse sections at the three sampling times. Image patch size was consistent for all evaluated magnifications (414 μm × 414 μm). The gray level co-occurrence matrix (GLCM) extracted textural features from the images, representing the relationships between pairs of adjacent pixels in a specific direction and distance (Davies, 2018). The texture parameters (angular second moment (ASM), contrast, correlation, inverse difference moment (IDF), and entropy) of the SEM images were evaluated using the GLCM and surface plot tools in ImageJ.

2.5. Statistical analysis

A one-way analysis of variance (ANOVA) was conducted to examine differences between treatments for chemical characterization (TPC, TFC, DPPH, ABTS) and the image analysis parameter (a^*, number of particles, size of particles, and area). The assumptions of normality (Shapiro-Wilk test), homoscedasticity (Levene's test), and independence (Durbin-Watson test) were verified before performing ANOVA to ensure the validity of the statistical analysis. The R^2 value was used to evaluate the goodness of fit of the model. The *p*-values were utilized to determine the significance of the model and identify statistically significant effects ($p < 0.05$). Tukey's multiple comparison post hoc test was employed to compare the control (SF) with each treatment sample.

3. Results and discussion

3.1. Chemical characterization

The results of assays to evaluate the total phenolic content (TPC), total tannin content (TTC), and antioxidant activities in cacao samples derived from controlled transformation and spontaneous fermentation are shown in Fig. 1. ANOVA revealed a significant effect of the transformation process on TPC and TTC ($p = < 2*10^{-16}$). The assumptions of normality ($p = 0.09134$ for TPC, $p = 0.5823$ for TTC), homoscedasticity ($p = 0.7426$, for TPC, $p = 0.7303$ for TTC), and independence ($p = 0.8892$ for TPC, $p = 0.7092$ for TTC) were verified, supporting the

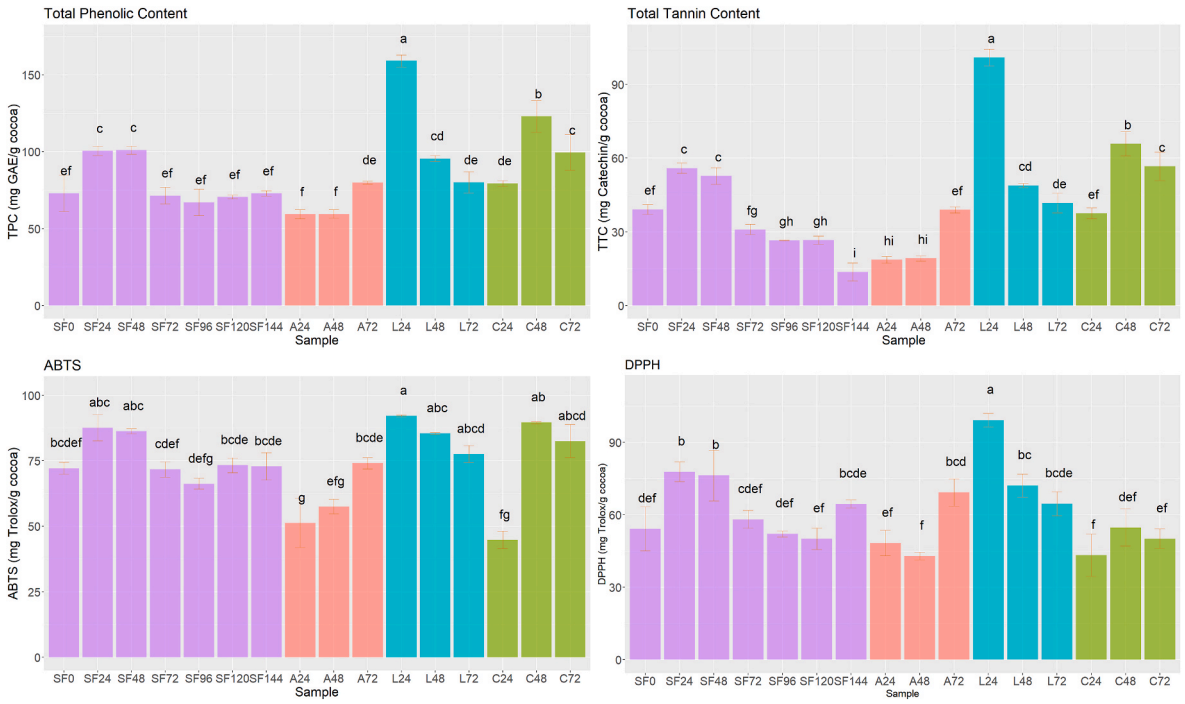

Fig. 1. A) Total phenolic content (mg GAE/g cacao). B) Total tannin content (mg catechin/g cacao). Antioxidant activity (mg Trolox/g cacao), measured by C) ABTS and D) DPPH assays throughout the controlled transformation of cacao seeds and during spontaneous fermentation. Values in the same graph with different lowercase letters are significantly different ($p < 0.05$). SF: Spontaneous Fermentation. A: acetic acid. L: lactic acid. C: citric acid.

robustness of the statistical analysis. The analysis of the spontaneous fermentation (SF) samples reveals a significant trend towards a decrease in total phenolic content (TPC) and total tannin content (TTC) as fermentation time increases. This behavior suggests that, during the process, phenolic compounds undergo degradation and polymerization, as well as interactions with proteins and other bioactive compounds, reducing their content (Brito et al., 2002; Febrianto and Zhu, 2020). Additionally, the antioxidant activity, evaluated through the ABTS and DPPH assays, also demonstrates a decline over time. This implies that, although there may be an initial increase in the release of compounds with antioxidant properties driven by microbial activity and favorable pH conditions that promote the enzymatic activity and chemical reactions, prolonged fermentation leads to a decrease in the content of these beneficial compounds. This phenomenon may be explained by the diffusion of compounds out of the seed, a process that, according to the obtained data, appears to commence after 24 h of transformation. This pattern highlights the importance of fermentation time on the stability of bioactive compounds, suggesting that an excessive period can be detrimental to preserving their antioxidant properties (Febrianto and Zhu, 2020).

In contrast, the analysis of samples obtained from the controlled transformation of cacao seeds did not reveal a consistent trend in the phenolic and tannin content across all treatments. The sample treated with lactic acid for 24 h (L24) exhibited the highest total phenolic content (159.09 ± 3.81 mg GAE/g cacao) and total tannin content (101.02 ± 3.47 mg CAT/g cacao). This finding supports with previous studies highlighting a greater content of phenolic compounds in samples treated with lactic acid (Becerra et al., 2023; Eyamo Evina et al., 2016). However, after 72 h of transformation, the values decreased to 80.07 ± 6.90 mg GAE/g cacao and 41.73 ± 4.09 mg CAT/g cacao. This trend underscores the adverse effects of prolonged transformation on the stability of these bioactive compounds when utilizing lactic acid.

Conversely, a different behavior is observed in the samples transformed with citric acid (CA) and acetic acid (AA). The seeds treated with citric acid exhibit higher total phenolic values (99.49 ± 11.61 mg GAE/g cacao) and total tannins (56.67 ± 5.80 mg CAT/g cacao) after 72 h of transformation. In these samples, the low pH of the cacao seeds (pH < 5) facilitates the maintenance of phenolic compounds in their protonated form, ensuring the stability of the compounds against oxidation (Saarniit et al., 2023). On the other hand, the phenolic and tannin content in the samples transformed with acetic acid is lower than that observed in samples treated with lactic and citric acids. Nevertheless, treatments with organic acids contribute to a statistically significant enhancement in the content of these bioactive compounds in cacao compared to the results obtained from spontaneous fermentation. Remarkably, at the end of spontaneous fermentation, the lowest levels of total phenolic content (72.89 ± 1.78 mg GAE/g cacao) and total tannin content (13.64 ± 3.74 mg CAT/g cacao) are observed.

The changes in phenolic and tannin content may be attributed to the processing steps of cacao seeds, particularly the drying step. This step is crucial for removing excess moisture and enabling a targeted extraction of phenolic compounds. The drying process, typically conducted at 50 °C, promotes greater evaporation of acetic acid, which is more volatile than lactic and citric acids. This differential volatility allows for the retention of the latter acids, which impart a lower internal pH to the seeds, a critical factor in preserving the integrity of phenolic compounds (Andrés-Bello et al., 2013). Moreover, these organic acids facilitate the breakdown of plant cell walls, enhancing the release of polyphenols (Renard et al., 2017). This effect is especially important in plant materials with dense cellular structure, such as cacao, as the acids can effectively decompose the matrix that retains phenolic compounds, thereby increasing their bioavailability.

The content of phenolic compounds and tannins showed a positive correlation with the antioxidant activity displayed by the cacao samples. ANOVA revealed a significant effect of the transformation process on ABTS and DPPH ($p = 5.56*10^{-10}$ for ABTS, $p = 1.89*10^{-12}$ for DPPH). The assumptions of normality ($p = 0.87053$ for ABTS, $p = 0.8689$ for DPPH), homoscedasticity ($p = 0.3924$, for ABTS, $p = 0.8664$ for DPPH), and independence ($p = 0.7916$ for ABTS, $p = 0.9808$ for DPPH) were verified, supporting the robustness of the statistical analysis. In the ABTS and DPPH assays, the sample treated with lactic acid (L24) exhibited the highest antioxidant activity, reaching approximately 90 mg Trolox/g

cacao in both tests (Fig. 1). Samples treated with citric acid also demonstrated significant antioxidant activity, reinforcing the influence of acid treatments on enhancing the antioxidant properties of cacao. These findings align with existing literature, indicating that higher phenolic content enhances antioxidant capacity (Borja Fajardo et al., 2022; Deus et al., 2021; Lima et al., 2024). In contrast to the quantification results, the antioxidant activity of the samples from controlled transformation showed minimal differences compared to those from spontaneous fermentation. These results underscore the significance of transformation conditions (temperature, OA concentration) in optimizing the quality of cacao concerning its bioactive compound composition.

It is important to note that phenolic compounds and condensed tannins are crucial as they contribute to the bitterness and astringency of cacao beans. A previous study (Becerra et al., 2024) reported that chocolate made from cacao seeds transformed with acetic acid exhibits a sensory profile characterized by its global quality and nutty notes alongside the typical flavor and aroma of cacao. This sensory experience is made possible by the lower contribution of bitter and astringent notes, resulting from the reduced content of phenolic compounds and condensed tannins. Consequently, this reduction allows the flavor and aroma characteristics developed in the subsequent stages of transformation from beans to chocolate to be more prominently highlighted.

3.2. Autofluorescence analysis of cacao seed microstructure using CLSM

Fig. 2 shows both transverse and longitudinal sections of cacao seeds from the three trials (AA, LA, CA) at three sampling times (24 h, 48 h, 72 h), as well as the spontaneous fermentation (SF) at three sampling times (48 h, 96 h, and 144 h). A high density of colored structures is observed, exhibiting a noticeably higher color intensity than other seed structures. Without chemical staining processes, the observed fluorescence is attributed to specific chemical compounds within the seed structures (Razgonova et al., 2022). These compounds were detected in the spectral region between 600 and 720 nm, where various autofluorescent molecules, such as flavonoids and tannins, typically coexist (García-Plazaola et al., 2015).

Among these compounds, anthocyanins, a subgroup within flavonoids, are particularly intriguing due to their ability to impart the characteristic purple hue to cacao seeds. It has been reported that these compounds exhibit red fluorescence when exposed to acidic conditions (Gomez et al., 2011). Therefore, this coloring can be primarily attributed

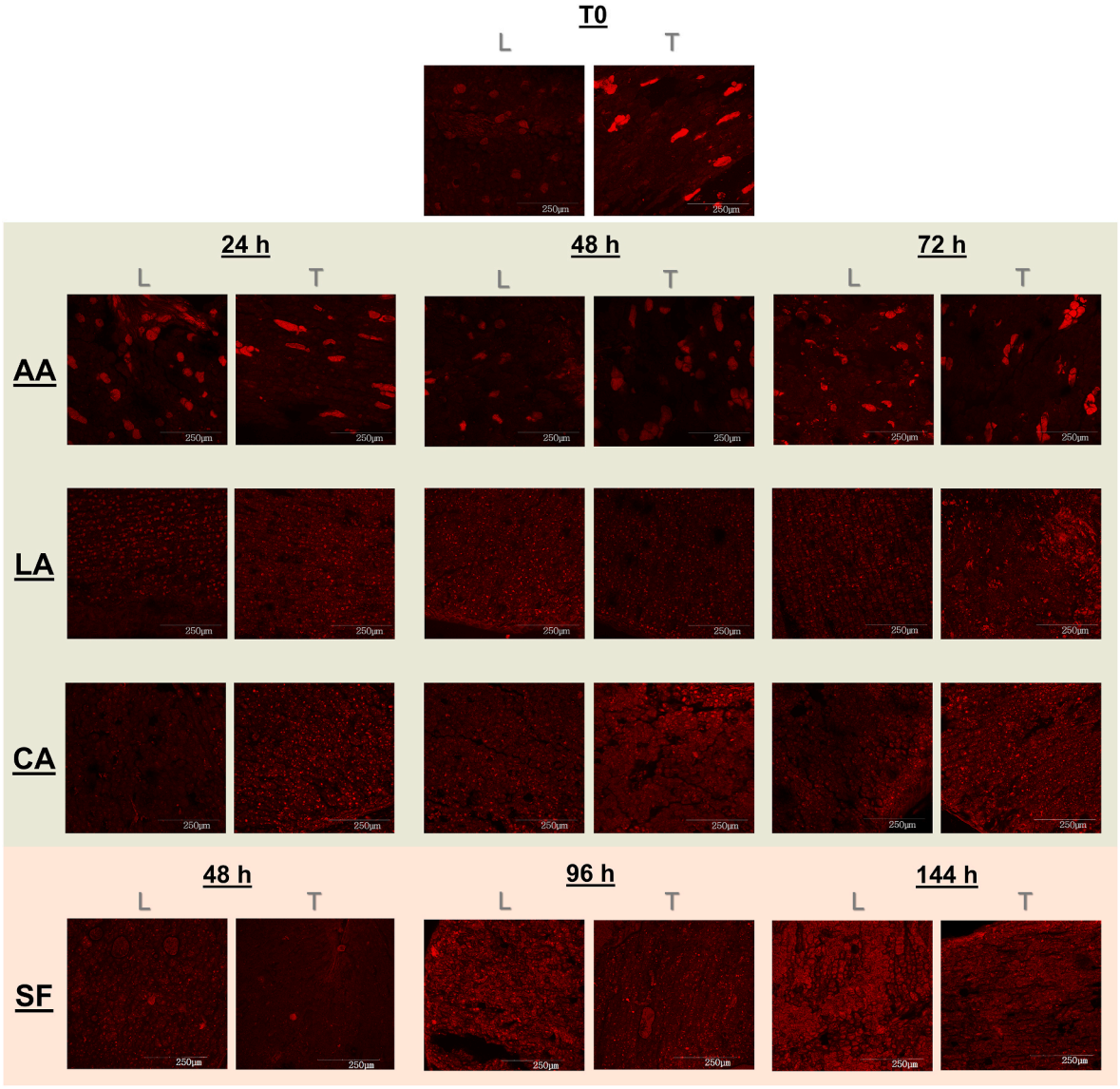

Fig. 2. CLSM images of autofluorescence of cacao seeds during controlled transformation and spontaneous fermentation (SF). AA: acetic acid, LA: lactic acid, CA: citric acid. L: longitudinal, T: transversal. T0: Raw seeds.

to the accumulation of anthocyanins within large vacuoles, compartmentalized in vesicle-like structures of varying sizes. Given the strong association of anthocyanins with the natural production of red autofluorescence in numerous plant species (Poobathy et al., 2018), the quantification of the red color using the a^* color parameter is presented in Table 2. ANOVA revealed a significant effect of the transformation process on a^* color parameter ($p < 2*10^{-16}$). The assumptions of normality ($p = 0.85475$), homoscedasticity ($p = 0.5877$), and independence ($p = 0.1688$) were verified, supporting the robustness of the statistical analysis.

In the control group (T0), phenolic vesicles display a spherical shape in longitudinal sections and an elongated, irregular shape in transverse sections, occupying a significant portion of the vacuole's space. As summarized in Table 2, raw seeds (T0) demonstrated an a^* value of 14.99 ± 3.06 in the longitudinal section and 21.15 ± 1.55 in the transverse section, indicating initial differences in the colorimetric parameter between both sections, with the transverse section displaying a higher value attributed to its larger exposed surface area. ANOVA indicated a significant influence of the transformation process on the number of particles ($p = 0.00469$). The validity of the analysis was confirmed by meeting the assumptions of normality ($p = 0.6569$), homoscedasticity ($p = 0.8514$), and independence ($p = 0.1868$), ensuring the reliability of the statistical results. The quantification of vesicles revealed relatively low particle counts, with 261 ± 120 in the longitudinal section and 196 ± 74 in the transverse section, suggesting a more compact structural arrangement of polyphenolic cells before any treatment. Regarding size, the particles exhibited considerable dimensions, with 122.81 ± 103.94 μm in the longitudinal section and 119.297 ± 35.15 μm in the transverse section, indicating that the original samples contained large vesicles before the controlled transformation. ANOVA showed a significant effect of the transformation process on particle size ($p = 0.00424$). The reliability of the statistical analysis was confirmed by fulfilling the assumptions of normality ($p = 0.7672$), homoscedasticity ($p = 0.1565$), and independence (p = 0.3501).

Table 2
Parameter values for CLSM-acquired images of longitudinal and transversal sections of cacao seeds transformed with acetic acid (AA), lactic acid (LA), and citric acid (CA) for 24 h, 48 h, and 72 h.

	Trial	a^*	Number of Particles	Size
Longitudinal sections	**T0**	14.99 ± 3.06^{a}	261 ± 120^{e}	122.81 ± 103.94^{b}
	A24	9.71 ± 1.99^{b}	98 ± 25^{e}	289.51 ± 31.90^{a}
	A48	10.5 ± 2.66^{b}	149 ± 41^{e}	111.29 ± 7.32^{bc}
	A72	17.43 ± 3.85^{a}	184 ± 32^{e}	91.447 ± 38.76^{bc}
	L24	15.79 ± 1.24^{b}	1101 ± 196^{cde}	41.43 ± 11.72^{bc}
	L48	21.71 ± 1.56^{a}	1466 ± 326^{bcd}	18.95 ± 4.27^{c}
	L72	19.03 ± 3.09^{a}	1978 ± 362^{bc}	24.11 ± 4.31^{bc}
	C24	6.75 ± 1.76^{c}	741 ± 302^{de}	19.25 ± 4.66^{c}
	C48	26.24 ± 2.18^{a}	3159 ± 1113^{a}	15.48 ± 4.80^{c}
	C72	16.69 ± 2.79^{b}	2345 ± 241^{ab}	8.41 ± 2.39^{c}
Transversal sections	**T0**	21.15 ± 1.55^{a}	196 ± 74^{c}	119.297 ± 35.15^{ab}
	A24	16.47 ± 3.62^{b}	93 ± 68^{c}	231.25 ± 223.06^{ab}
	A48	8.48 ± 1.07^{c}	100 ± 55^{c}	340.43 ± 231.02^{a}
	A72	24.56 ± 5.26^{a}	74 ± 30^{c}	269.89 ± 118.19^{ab}
	L24	21.32 ± 1.57^{a}	1583 ± 598^{ab}	19.21 ± 2.52^{b}
	L48	14.37 ± 2.02^{b}	1432 ± 241^{b}	21.66 ± 4.50^{b}
	L72	20.59 ± 2.19^{a}	1651 ± 24^{ab}	27.83 ± 5.29^{ab}
	C24	18.57 ± 1.68^{b}	2663 ± 153^{a}	14.56 ± 1.51^{b}
	C48	24.41 ± 3.03^{a}	2781 ± 714^{a}	11.38 ± 4.76^{b}
	C72	24.27 ± 2.35^{a}	2209 ± 897^{ab}	10.32 ± 1.36^{b}

Values are means ± standard deviation (n = 10). Means with different letters in the same column and section indicate a significant statistical difference ($p < 0.05$).

General trends emerge when comparing longitudinal and transverse sections of cacao seeds during their controlled transformation with acetic acid. The a^* parameter reveals significant differences ($p < 0.05$) between the control group and seeds transformed for 24 and 48 h in both sections. However, no significant differences were observed between the control group and seeds transformed for 72 h. As transformation progresses, a decrease in the number of vesicles and a concurrent increase in their size is observed. However, there are no statistical differences with T0. This observation suggests that acetic acid, with a pKa of 4.76, may favor the stability of the vesicles through electrostatic interactions with the surrounding membrane (Renard et al., 2017). Such interactions could enhance vesicle cohesion, thereby preventing disaggregation and contributing to the formation of larger structures. This is consistent with the literature, which indicates that maintaining a stable pH environment is crucial for the integrity of phenolic vesicles during transformations in plant cells (Mackon et al., 2021).

Previous studies by Elwers et al. (2010) indicated that the larger polyphenol and storage cells found in Criollo cacao seeds may significantly contribute to the distinctive quality of this fine-flavor cacao, particularly when contrasting various cacao varieties, including bulk cacao. This finding is consistent with the current research, which demonstrates that treatment with acetic acid—previously associated with fine-flavor cacao—also promotes the formation of larger vesicles containing polyphenols. Furthermore, the implications of these structural changes in vesicle size and quantity may play a crucial role in the overall phenolic profile and sensory attributes of the cacao, highlighting the importance of treatment conditions in optimizing cacao quality.

In contrast, seeds treated with lactic acid and citric acid exhibit a high density of vesicles in both sections. Compared to the control group, anthocyanin inclusions were smaller ($p < 0.05$) and occupied less vacuole space. These structures displayed a uniform distribution within the tissue, with no significant differences between transformation times. For LA and CA trials, the a^* parameter in transverse sections remained relatively constant, except for the 48-h treatment in the longitudinal section, which showed higher values. Notably, these treatments disrupted vesicles, forming much smaller structures than those in T0 and AA. Additionally, a red coloration outside the vesicles was observed, likely due to anthocyanin diffusion into the vacuolar space (Mackon et al., 2021).

The formation of polyphenolic vesicles during cacao seed transformation has not been extensively studied. However, evidence from other plants suggests that vacuolar proteins exhibit a strong affinity for acylated anthocyanins, leading to anthocyanic vacuolar inclusions (AVIs) (H. Zhang et al., 2006). This interaction, influenced by pH, involves electrostatic interactions, hydrogen bonding, and protein conformational changes. Acetic, lactic, and citric acids are weak acids that can passively diffuse into cells until an equilibrium is reached across the membrane. Once in the cytosol, these acids dissociate, releasing protons and causing a decrease in intracellular pH (Bai et al., 2006). Subsequently, the protons are transported to the vacuoles, creating potential energy and pH gradients both inside and outside the vacuoles. These conditions facilitate the transport of organic acids (Huang et al., 2021). At the vacuolar pH, the protein-anthocyanin interaction is robust, and the proteins effectively trap anthocyanins (Markham et al., 2000). However, during the controlled transformation of cacao seeds, the acidic cytosolic pH positively correlates with the vacuolar pH (Deguchi et al., 2020), which changes these interaction mechanisms.

The observed similarity in behavior between the LA and CA treatments is remarkable. The lowest pH values were observed in citric acid trials, followed by lactic and acetic acids (Becerra et al., 2023). Acetic acid, lactic acid, and citric acid have been employed in the extraction of anthocyanins from plants due to their ability to facilitate vacuole

fragmentation, leading to the disruption of cell membranes (Gokbayrak et al., 2022; Nunes et al., 2022). This behavior is attributed to stabilizing the cationic form of flavylium, enhancing both the extraction efficiency and the stability of anthocyanins, with optimal stability observed at pH < 3 (Galvão et al., 2020). Furthermore, it is observed that CLSM images (Fig. 2) exhibit greater color intensity at lower pH values, as evidenced by seeds treated with lactic acid and citric acid compared to those treated with acetic acid. This suggests that the higher pH in seeds transformed with acetic acid does not favor the disruption of the original vesicles, thus maintaining their original form.

Despite employing different concentrations of the respective organic acid, both treatments, LA and CA, share the use of a temperature of 45 °C during the controlled transformation process. This temperature can induce stress responses in cells, resulting in alterations in cell membrane structure, protein denaturation, compromised functionality, and increased membrane fluidity and permeability (Zhao et al., 2020). In contrast, the AA treatment, which employs a temperature of 30 °C, did not exhibit these effects. Consequently, this operating variable could significantly influence the microstructural changes during the seed's transformation process.

3.3. SEM characterization of cacao seed microstructure

The microstructural changes in cacao seeds during controlled transformation were assessed using SEM, as shown in Fig. 3. The cotyledon, consisting of parenchymal cells, displayed a compact arrangement in all treatment groups. Representative images in Fig. 3 illustrate the various cellular components and internal structures observed. The cell walls appeared thin and were storage sites for essential compounds such as lipids, starch, proteins, and phenolic compounds. These compounds are essential precursors for flavor development in subsequent chemical reactions.

When the seeds were treated with acetic acid (1 g/L), noticeable changes were observed in the structure of the cell walls. Acetic acid, upon dissociation, disrupts the ionic balance within the cell wall, significantly affecting its structure and functionality (Y. Zhang et al., 2020). Fig. 3 shows the changes in cell volume of the seeds treated with acetic acid, which can be attributed to the osmotic stress induced by the organic acid. As a consequence, acetic acid can potentially increase membrane permeability, facilitating the inward diffusion of the acid into the cells (Bai et al., 2006). It has been reported that acetic acid has a more significant impact on membrane permeability than citric acid (Bai et al., 2006). Unlike acetic acid, citric acid is an intermediate in several metabolic pathways, and plant cells have mechanisms for its transport and reuse. Therefore, its regulation prevents damage to the tonoplast (Huang et al., 2021). It is important to note that the strength of the acid, its molecular structure, and potential chemical interactions with cellular components contribute to the resulting cellular damage.

These observations align with previous studies focusing on the controlled transformation of cacao seeds, which have consistently reported more significant cell damage with acetic acid (Biehl et al., 1982). Additionally, recent research by Becerra et al. (2022) supports these findings by indicating that acetic acid diffuses more rapidly in cacao seeds than lactic acid and citric acid. Moreover, the controlled transformation of cacao seeds with acetic acid has been linked to distinctive flavor and aroma profiles. This behavior can be attributed to increased cellular damage, which enhances the availability of endogenous components in the seeds that participate in the chemical reactions responsible for flavor development.

The formation of intercellular spaces (IS) can be observed in the

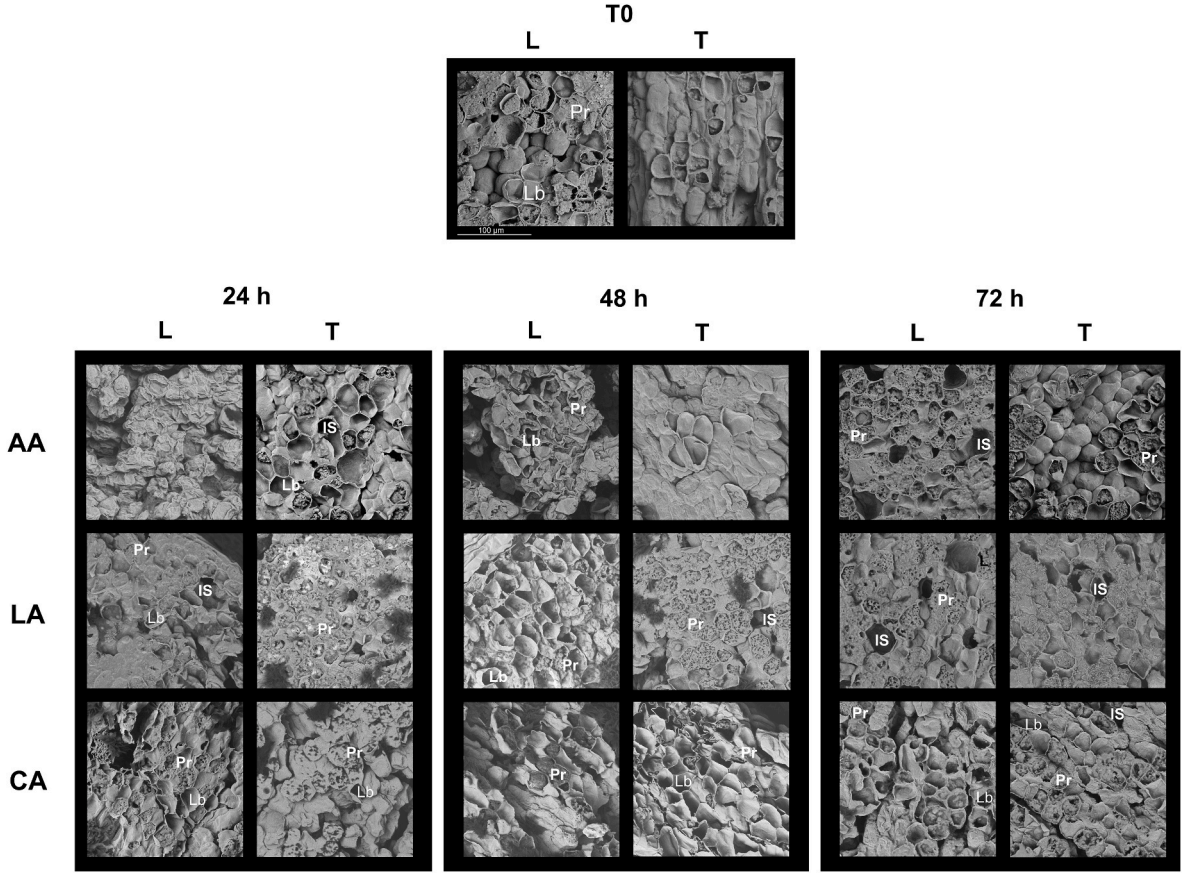

Fig. 3. SEM images of longitudinal (L) and transversal (T) sections of cacao seeds during controlled transformation with AA: acetic acid, LA: lactic acid, and CA: citric acid. T0: Raw seeds. The white bar indicates the scale. Magnification: 1000×. IS: Intercellular space, Pr: Protein, Lb: Lipid bodies.

cotyledon of cacao seeds (Fig. 3). This phenomenon is particularly pronounced in longitudinal sections of the seeds after 72 h of transformation with acetic acid and lactic acid, as shown in Fig. 3. CLSM revealed a similar occurrence in seeds transformed with citric acid (Fig. 2). In contrast, these intercellular spaces were not detected in the control group seeds (T0). The formation of these cavities can be attributed to the diffusion of organic acids, which induce partial disintegration of the cell wall in these specific areas through chemical interactions with its components or by creating favorable conditions for enzymatic activity.

In the central region of the cells, protein reserves were observed, constituting the major portion of the cytoplasmic network (Fig. 3). However, due to the alcoholic dehydration method employed for SEM analysis, lipid bodies appear as empty spaces within the cells. Both protein reserves and lipid bodies are visible in all treatments. Phenolic compound cells were not visible at 1000× magnification. However, at 5000× magnification, phenolic compound aggregates became visible in the organic acid treatments after 48 h of transformation indicating the presence of these compounds at higher concentrations in response to the organic acid treatments (Fig. 4). Among the organic acids used, the lactic acid treatment exhibited more phenolic compound aggregates than the other acids. Although the current analysis does not provide a comprehensive understanding of the protective pathway of lactic acid against phenolic compounds, the SEM findings support previous research indicating that controlled transformation under specific conditions using lactic acid at a concentration of 1 g/L, results in a high content of methylxanthines and flavan-3-ols in cacao beans (Becerra et al., 2023).

3.3.1. Texture analysis

A texture analysis was conducted to obtain quantifiable parameters from the SEM-acquired images (Fig. 3). Visual textures typically arise from the interaction between light and a rough surface (Yoshimizu et al., 2022). Data is encoded in a digital surface representation as a pixel matrix with different intensity levels or grayscale values. The localized fluctuations in brightness between adjacent pixels or within a small region are commonly referred to as texture (Quevedo et al., 2002). In this study, a second-order statistical method, the gray-level co-occurrence matrix, was employed to describe the texture of cacao seeds during their controlled transformation (Ramola et al., 2020). Six texture parameters were obtained from the images: fractal dimension, angular second moment, contrast, correlation, inverse difference moment, and entropy (Table 3). The statistical analysis was performed by grouping the data according to the analyzed section (L, T) for images acquired at a magnification of 1000×, as it allows for better observation of cellular damage at smaller scales.

Statistically significant differences ($p < 0.05$) were observed when analyzing the fractal dimension of texture (FDt) in the micrographs of cacao seeds. Based on the findings from the transverse section, the seeds can be categorized into three subsets: the first subset corresponds to the control seeds, the second subset includes the images of seeds transformed with citric acid for 48 h, and the remaining treatments form the third subset. The CA48 treatment exhibited the lowest FDt values, indicating more homogeneous surfaces with greater uniformity and regularity in texture. Additionally, this treatment showed cuts that revealed empty spaces corresponding to lipid residues. This result is supported by higher values of the angular second moment (ASM) in both analyzed sections (L, T). The other treatments displayed higher variation and discontinuities in texture, as indicated by slightly lower ASM values.

When measuring the difference or variation between the light and dark areas of the image, it was found that the contrast textural feature presented lower values for the CA48 treatment in both analyzed sections. This indicates lower intensity variation and a more uniform texture (Mello Román et al., 2019). The longitudinal and transverse sections of the samples treated with acetic acid and lactic acid showed intermediate values; no significant difference was observed between them. In contrast, the control group exhibited the highest contrast value, indicating high local variation typical of heterogeneous surfaces. This result correlates with a greater diversity of cellular components (proteins, starch, and phenolic compounds) that have not been modified by the presence of the organic acids used in the controlled transformation. However, the cutting direction of the fresh seeds affected this parameter, resulting in a more uniform texture in the transverse section due to the cellular packing of the cotyledon.

Correlation is a textural parameter used to measure the similarity or linear relationship between the grayscale levels or colors of adjacent pixels in an image (Mirjalili and Hardeberg, 2022). Its range is between −1 and +1, and all presented positive values close to zero for the treatments analyzed here. Therefore, although significant differences were observed among the treatments, the parameter's numerical value indicates no correlation among the pixels in the images.

When analyzing the texture of the seeds using the Inverse Difference Moment (IDF) textural parameter, which measures the uniformity or variation of intensity values in an image, differentiation of the CA48 treatment was again observed in both analyzed sections. High IDF values can be associated with homogeneous images (Barrera et al., 2013). The treatments with acetic acid and lactic acid resulted in varied and irregular textures to the same extent, and no effect of processing time was observed on the parameter. For the control group, there was again a marked difference depending on the analyzed section, as occurred with the contrast of the images, with the structure of the transverse section being homogeneous.

Finally, the statistical analysis of the results revealed a significant difference ($p < 0.05$) among the treatments when analyzing the entropy of the micrographs. Entropy quantifies the randomness or lack of information in the distribution of grayscale levels in a texture (Mello Román et al., 2019). The more uniform or random the distribution of grayscale levels, the lower the entropy, as seen in the CA48 treatment. Additionally, regarding the cellular packing of the cotyledon tissue

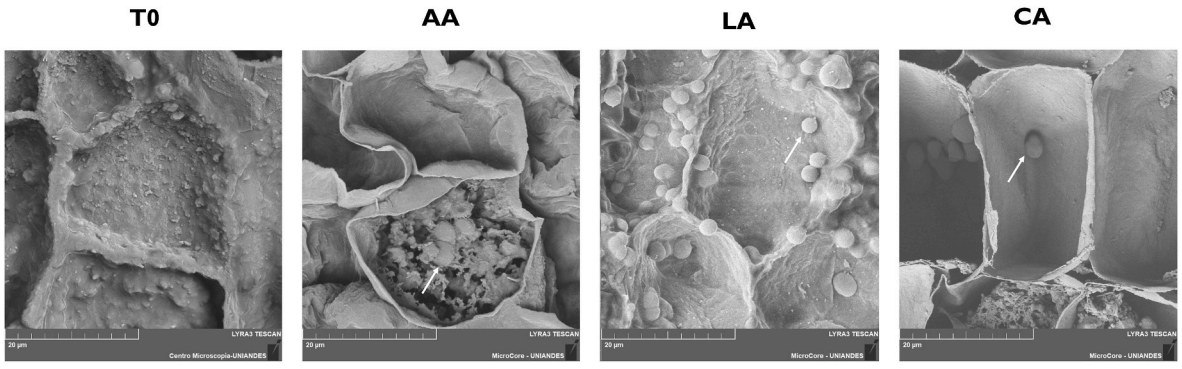

Fig. 4. Scanning electron micrographs at 5000x of raw (T0) and transformed seeds with acetic acid (AA), lactic acid (LA), and citric acid (CA) during 48 h. Polyphenolic compound aggregates are shown (white arrow).

Table 3
Texture parameters for SEM-acquired images at 1000x.

Section	Sample	FDt	ASM	Contrast	Correlation	IDF	Entropy
L	T0	2.602 ± 0.020^{a}	8.89E-05 ± 8.31E-06 ^{b}	664.6 ± 116.5^{a}	3.49E-04 ± 5.57E-05^{b}	0.072 ± 0.008^{c}	9.709 ± 0.108^{a}
L	A24	2.535 ± 0.016^{ab}	1.23E-04 ± 1.01E-05 ^{b}	366.3 ± 33.4^{bc}	3.89E-04 ± 1.03E-05^{b}	0.095 ± 0.006^{bc}	9.355 ± 0.119^{ab}
L	A48	2.525 ± 0.042^{b}	1.52E-04 ± 7.85E-05 ^{b}	429.4 ± 118.4^{b}	3.91E-04 ± 7.07E-05^{b}	0.091 ± 0.018^{bc}	9.352 ± 0.213^{ab}
L	A72	2.514 ± 0.026 ^{b}	1.73E-04 ± 3.01E-05 ^{b}	230.2 ± 39.5^{cd}	5.99E-04 ± 2.74E.04^{ab}	0.109 ± 0.023^{b}	9.021 ± 0.187^{b}
L	L24	2.477 ± 0.006 ^{b}	1.81E-04 ± 2.58E-05 ^{b}	249.9 ± 17.7^{bcd}	6.53E-04 ± 1.97E-04^{ab}	0.097 ± 0.009^{bc}	8.986 ± 0.131^{b}
L	L48	2.518 ± 0.035 ^{b}	1.59E-04 ± 7.64E-05 ^{b}	332.3 ± 61.7^{bcd}	3.90E-04 ± 5.50E-05^{b}	0.101 ± 0.018^{bc}	9.267 ± 0.256^{ab}
L	L72	2.491 ± 0.049 ^{b}	1.52E-04 ± 4.15E-05 ^{b}	300.8 ± 108.5^{bcd}	5.34E-04 ± 1.49E-04^{ab}	0.094 ± 0.012^{bc}	9.156 ± 0.292^{b}
L	C24	2.527 ± 0.033 ab	1.48E-04 ± 3.44E-05 ^{b}	418.9 ± 110.8^{bc}	3.90E-04 ± 1.73E-04^{b}	0.099 ± 0.011^{bc}	9.355 ± 0.258^{ab}
L	C48	2.501 ± 0.035 ^{b}	4.94E.04 ± 9.17E-06^{a}	148.2 ± 29.9^{d}	7.89E-04 ± 1.88E-04^{a}	0.161 ± 0.024^{a}	8.343 ± 0.288^{c}
L	C72	2.534 ± 0.024^{ab}	1.08E-04 ± 9.17E-06 ^{b}	381.0 ± 80.9^{bc}	3.58E-04 ± 2.42E-05^{b}	0.085 ± 0.010^{bc}	9.439 ± 0.100^{ab}
T	T0	2.454 ± 0.036 ^{b}	2.15E-04 ± 3.56E-05^{ab}	207.9 ± 46.3^{c}	7.08E-04 ± 1.58E-05^{a}	0.114 ± 0.004^{a}	8.832 ± 0.133^{c}
T	A24	2.559 ± 0.019^{a}	1.06E-04 ± 8.95E-06^{c}	480.8 ± 60.0^{a}	3.08E.04 ± 3.78E-05^{c}	0.079 ± 0.004^{b}	9.583 ± 0.080^{a}
T	A48	2.521 ± 0.019^{a}	1.48E-04 ± 3.14E-05^{bc}	365.9 ± 74.6^{ab}	4.57E-04 ± 1.63E-05^{abc}	0.089 ± 0.006^{b}	9.255 ± 0.196^{ab}
T	A72	2.539 ± 0.050^{a}	1.53E-05 ± 3.99E-05^{bc}	352.9 ± 102.4^{ab}	4.43E-04 ± 1.49E-05^{bc}	0.110 ± 0.013^{a}	9.267 ± 0.291^{ab}
T	L24	2.519 ± 0.013^{a}	1.49E-04 ± 4.36E-05^{bc}	375.7 ± 50.4^{ab}	5.50E-04 ± 1.69E-05^{abc}	0.075 ± 0.008^{b}	9.252 ± 0.143^{ab}
T	L48	2.514 ± 0.015^{a}	1.38E-04 ± 1.56E-05^{bc}	393.9 ± 14.5^{ab}	5.10E-04 ± 9.82E-05^{abc}	0.077 ± 0.006^{b}	9.237 ± 0.085^{ab}
T	L72	2.516 ± 0.015^{a}	1.37E.04 ± 1.74E-05^{c}	371.6 ± 60.7^{ab}	6.14E-04 ± 1.08E-05^{ab}	0.079 ± 0.009^{b}	9.222 ± 0.102^{b}
T	C24	2.527 ± 0.010^{a}	1.25E-04 ± 7.261E-06^{c}	392.1 ± 41.6 ab	4.52E-04 ± 3.82E-05^{abc}	0.072 ± 0.002^{b}	9.269 ± 0.068^{ab}
T	C48	2.507 ± 0.019^{ab}	2.59E-04 ± 6.40E-05^{a}	321.5 ± 51.4^{bc}	3.68E-04 ± 3.02E-05^{bc}	0.126 ± 0.009^{a}	9.068 ± 0.123^{bc}
T	C72	2.534 ± 0.019^{a}	1.19E-04 ± 8.81E-06^{c}	351.2 ± 36.6^{ab}	4.21E-04 ± 7.34E-05^{bc}	0.086 ± 0.005^{b}	9.353 ± 0.082^{ab}

observed in the control group seeds, higher entropy can be observed when subjecting the seeds to the process of transformation with organic acids, suggesting that controlled seed transformation increases entropy. Hence, entropy seems to be a proper textural parameter for numerically describing microstructural changes.

Trial CA has been previously associated with producing cacao matrices exhibiting red-pink color hues. While this coloration is observed in transformed cacao beans, the cacao husk has a more prominent presence of this color characteristic (Becerra et al., 2023). Therefore, further research is needed to investigate husk structures' behavior and extensively study the influence of structural changes on cacao quality parameters. Understanding these relationships will provide valuable insights into the impact of structural modifications on the overall quality of cacao.

3.4. Relationship between CSLM-image parameters, bioactive compound content, and antioxidant activity

The observed correlations between chemical characteristics and image parameters obtained through CSLM analysis reveal meaningful relationships when applying Pearson correlation as a measure of linear dependence to SF data (Fig. 5A). The results suggest a strong positive relationship between total polyphenol content (TPC) and antioxidant activity, with correlations of 0.91 in the DPPH assay and 0.98 in the ABTS assay. This is consistent with the fact that polyphenols are potent antioxidants that neutralize free radicals.

Regarding total tannin content (TTC), the moderate correlation with antioxidant activity measured by ABTS (0.71) indicates that while tannins contribute to antioxidant capacity, their impact is not as pronounced as that of polyphenols. Notably, a significant negative correlation was found between total tannin content and particle area (−0.98), as well as with the color parameter α * (−0.96). This suggests that total tannin content increases as particle area decreases and α* values (which indicate red hue) are reduced. This phenomenon may be related to the formation of anthocyanin vacuolar inclusions (AVIs) in the cellular space, resulting from changes induced during the transformation of cacao seeds. The formation of these structures affects the occupied area and presents a geometric advantage: AVIs, characterized

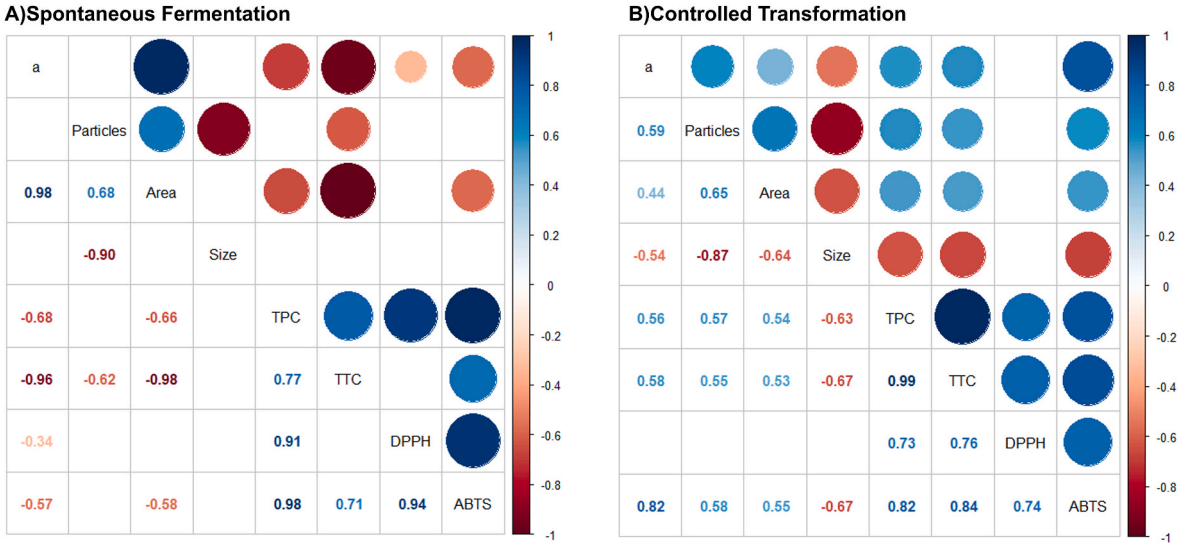

Fig. 5. Pearson correlation between CSLM image parameters (a^{*}, number of particles, area, size), bioactive compound content (TPC, TTC), and antioxidant activity (DPPH, ABTS) for A) spontaneous fermentation and B) controlled transformation of cacao seeds. The color scale represents correlation coefficients, ranging from −1 (red, strong negative correlation) to +1 (blue, strong positive correlation). Values close to 0, indicating no linear correlation, are shown in white. (For interpretation of the references to color in this figure legend, the reader is referred to the Web version of this article.)

by their small size, have a relatively larger surface area than their volume. This geometric feature enhances the efficiency of anthocyanin extraction processes by increasing the contact surface between extraction solvents and phenolic compounds within the cellular matrix. As a result, tannin recovery is optimized, contributing to the increase in tannin content in the final extract. In this context, the significant relationship between the reduced size of AVIs and the increase in tannin content is evident. Therefore, image parameters provide an indirect method for predicting tannin content and a visual representation of the chemical and structural modifications occurring in cacao during its transformation. This dual utility of image parameters underscores their importance in the characterization and optimization of extraction processes in cacao studies.

Based on the correlations observed from the data obtained during the spontaneous fermentation of cacao seeds (Fig. 5A), a linear model was proposed to predict the total tannin content (TTC) from the area occupied by autofluorescent structures Table 4. The model proved to be statistically significant ($p < 0.05$) with a high coefficient of determination ($R^2 = 0.9549$), indicating that a substantial proportion of the variability in TTC can be explained by variations in the area occupied by anthocyanins. Furthermore, the Studentized Breusch-Pagan test revealed a p-value >0.05 (0.9748), suggesting no issues of heteroscedasticity in the model estimates. Similarly, the Shapiro-Wilk normality test yielded a p-value >0.05 (0.4302), confirming that the model's residuals are normally distributed, thus meeting a fundamental assumption of linear regression. These results support the model's validity and ability to reliably predict total tannin content based on the area of autofluorescent structures.

For the data obtained after the controlled transformation of cacao seeds, Pearson correlation analysis (Fig. 5B) revealed significant relationships between the studied variables, notably a strong positive correlation between total phenolic content (TPC) and total tannins (TTC) ($r = 0.988$, $p < 0.05$), suggesting that an increase in phenolic compounds is directly associated with a rise in tannin levels. Additionally, significant positive correlations were observed between TPC and antioxidant capacities measured by the ABTS ($r = 0.817$, $p < 0.05$) and DPPH ($r = 0.731$, $p < 0.05$) assays, indicating that higher phenolic content translates into greater antioxidant capacity. A notable negative correlation was also identified between particle size and particle number ($r = -0.87$).

Finally, a strong positive correlation was observed between the color parameter a^*, and the antioxidant capacity measured by the ABTS assay ($r = 0.818$, $p < 0.05$). For this latter correlation, a linear model was developed that, although statistically significant, exhibited a low predictive power ($R^2 = 0.6691$), suggesting that while the red hue of the samples is related to their antioxidant capacity, other factors also influence this relationship, limiting the model's predictive capacity. This outcome underscores the impact of controlled transformation on phenolic compound content, where diffusion emerges as one of the most significant mass transfer phenomena. During this process, the surrounding incubation solution facilitates the release of phenolic compounds from within cellular structures to the external medium. This diffusional phenomenon occurs to a greater extent during controlled transformation than spontaneous fermentation, adding complexity to the simulation of the observed results.

4. Conclusions

The results indicate that the controlled transformation of cacao seeds using acetic, lactic, or citric acid significantly enhances the total phenolic and tannin content, as well as the antioxidant activity of the samples. These bioactive properties are critical for the quality of cacao and the development of high-quality products. Image analysis revealed notable microstructural changes in the cacao seeds, driven by the diffusion of organic acids used during the controlled transformation process. In the control group (T0), large vacuolar inclusions of anthocyanins, high structural homogeneity, and an abundance of intact protein bodies were observed. When transformed with acetic acid, the seeds exhibited no significant changes in the size of the vacuolar anthocyanin inclusions; however, an increase in membrane permeability and a reduction in cellular volume due to osmotic stress were noted. Conversely, seeds transformed with lactic acid displayed smaller vacuolar inclusions of anthocyanins, with phenolic cells being more prominent under scanning electron microscopy (SEM). This study represents pioneering research into the microstructure of cacao, aiming to open new avenues for understanding flavor formation using novel tools that have not been previously applied. It focuses on the relationship between microstructural changes and flavor precursors, which are critical in the development of quality-related characteristics, such as color, the presence of phenolic compounds, and the enhancement of desirable flavor and aroma notes in chocolate. Further research is needed to understand the full impact of microstructure on cacao quality, with advanced microscopy techniques offering valuable insights into structural modifications during transformation.

Table 4
Linear model parameters for predicting total tannin content (TTC) from the area of autofluorescent structures during spontaneous cacao seed fermentation.

R^2	Adjusted R^2	Residual Std. Error	F	p
0.97	0.9549	3.562	64.59	0.01513
Coefficients	Estimate	Std. Error	t	p
intercept	92.7167	7.6411	12.134	0.00672 **
Area	−0.001786	0.000222	−8.037	0.01513 *

Declaration of competing interest

The authors declare that they have no known competing financial interests or personal relationships that could have appeared to influence the work reported in this paper.

Acknowledgements

The authors express their gratitude to the Universidad de La Sabana for funding this research through the ING-226–2019 project and "Avanza un paso más hacia la Ultima Milla" call.

Data availability

Data will be made available on request.

References

Aguilera, J.M., 2005. Why food microstructure? J. Food Eng. 67 (1), 3–11. https://doi.org/10.1016/j.jfoodeng.2004.05.050.
Aguilera, J.M., 2022. Rational food design and food microstructure. Trends Food Sci. Technol. 122, 256–264. https://doi.org/10.1016/j.tifs.2022.02.006.
Andersson, M., Koch, G., Lieberei, R., 2006. Structure and function of the seed coat of *Theobroma cacao* L. and its possible impact on flavour precursor development during fermentation. J. Appl. Bot. Food Qual. 80 (1), 48–62.
Andrés-Bello, A., Barreto-Palacios, V., García-Segovia, P., Mir-Bel, J., Martínez-Monzó, J., 2013. Effect of pH on color and texture of food products. Food Eng. Rev. 5 (3), 158–170. https://doi.org/10.1007/s12393-013-9067-2.
Auty, M.A.E., 2013. 4 - confocal microscopy: principles and applications to food microstructures. In: Morris, En V.J., Groves, K. (Eds.), Food Microstructures. Woodhead Publishing, pp. 96–131. https://doi.org/10.1533/9780857098894.1.96.
Bai, B., Li, L., Hu, X., Wang, Z., Zhao, G., 2006. Increase in the permeability of tonoplast of garlic (*Allium sativum*) by monocarboxylic acids. J. Agric. Food Chem. 54 (21), 8103–8107. https://doi.org/10.1021/jf061628h.
Barbosa-Pereira, L., Guglielmetti, A., Zeppa, G., 2018. Pulsed electric field assisted extraction of bioactive compounds from cocoa bean shell and coffee silverskin. Food Bioprocess Technol. 11 (4), 818–835. https://doi.org/10.1007/s11947-017-2045-6.
Barišić, V., Kopjar, M., Jozinović, A., Flanjak, I., Ačkar, Đ., Miličević, B., Šubarić, D., Jokić, S., Babić, J., 2019. The chemistry behind chocolate production. Molecules 24 (17), 3163. https://doi.org/10.3390/molecules24173163.
Barrera, G.N., Calderón-Domínguez, G., Chanona-Pérez, J., Gutiérrez-López, G.F., León, A.E., Ribotta, P.D., 2013. Evaluation of the mechanical damage on wheat

starch granules by SEM, ESEM, AFM and texture image analysis. Carbohydr. Polym. 98 (2), 1449–1457. https://doi.org/10.1016/j.carbpol.2013.07.056.
Becerra, L.D., Quintanilla-Carvajal, M.X., Escobar, S., Ruiz, R.Y., 2023. Correlation between color parameters and bioactive compound content during cocoa seed transformation under controlled process conditions. Food Biosci. 53, 102526. https://doi.org/10.1016/j.fbio.2023.102526.
Becerra, L.D., Ruiz-Pardo, R., Vaillant, F., Zuluaga, M., Boulanger, R., Santander, M., Escobar, S., 2024. Modulating fine flavor cocoa attributes: impact of seed-to-bean transformation under controlled conditions on metabolite, volatile and sensory profiles. Food Res. Int. 196, 115109. https://doi.org/10.1016/j.foodres.2024.115109.
Becerra, L.D., Zuluaga, M., Mayorga, E.Y., Moreno, F.L., Ruíz, R.Y., Escobar, S., 2022. Cocoa seed transformation under controlled process conditions: modelling of the mass transfer of organic acids and reducing sugar formation analysis. Food Bioprod. Process. 136, 211–225. https://doi.org/10.1016/j.fbp.2022.10.008.
Biehl, B., Passern, D., Sagemann, W., 1982. Effect of acetic acid on subcellular structures of cocoa bean cotyledons. J. Sci. Food Agric. 33 (11), 1101–1109.
Borja Fajardo, J.G., Horta Tellez, H.B., Peñaloza Atuesta, G.C., Sandoval Aldana, A.P., Mendez Arteaga, J.J., 2022. Antioxidant activity, total polyphenol content and methylxantine ratio in four materials of *Theobroma cacao* L. from Tolima, Colombia. Heliyon 8 (5), e09402. https://doi.org/10.1016/j.heliyon.2022.e09402.
Brand-Williams, W., Cuvelier, M.E., Berset, C., 1995. Use of a free radical method to evaluate antioxidant activity. LWT - Food Sci. Technol. (Lebensmittel-Wissenschaft -Technol.) 28 (1), 25–30. https://doi.org/10.1016/S0023-6438(95)80008-5.
Brillouet, J.-M., Hue, C., 2017. Fate of proanthocyanidins and anthocyanins along fermentation of cocoa seeds (*Theobroma cacao* L.). J. Appl. Bot. Food Qual. 90, 141–146. https://doi.org/10.5073/JABFQ.2017.090.017.
Brito, E. S. de, García, N.H.P., Amâncio, A.C., 2002. Effect of polyphenol oxidase (PPO) and air treatments on total phenol and tannin content of cocoa nibs. Food Sci. Technol. 22, 45–48. https://doi.org/10.1590/S0101-20612002000100008.
Chen, W.-S., Yuan, S.-Y., Hsiao, H., Hsieh, C.-M., 2001. Algorithms to estimating fractal dimension of textured images. 2001 IEEE Int. Conf. Acoust., Speech, Signal Process. Proc. (Cat. No.01CH37221) 3, 1541–1544. https://doi.org/10.1109/ICASSP.2001.941226, 3.
Davies, E.R., 2018. Chapter 7—Texture analysis. In: Davies, En E.R. (Ed.), Computer Vision, fifth ed. Academic Press, pp. 185–200. https://doi.org/10.1016/B978-0-12-809284-2.00007-1.
de Brito, E.S., García, N.H.P., Gallão, M.I., Cortelazzo, A.L., Fevereiro, P.S., Braga, M.R., 2001. Structural and chemical changes in cocoa (*Theobroma cacao* L) during fermentation, drying and roasting. J. Sci. Food Agric. 81 (2), 281–288. https://doi.org/10.1002/1097-0010(20010115)81:2<281::AID-JSFA808>3.0.CO;2-B.
Deguchi, A., Tatsuzawa, F., Miyoshi, K., 2020. A blackish-flowered cultivar of Catharanthus roseus accumulates high concentrations of a novel anthocyanin with a unique feature of aggregation in weak acid solutions. Dyes and Pigments 173, 108001. https://doi.org/10.1016/j.dyepig.2019.108001.
Deus, V.L., Resende, L.M., Bispo, E.S., Franca, A.S., Gloria, M.B.A., 2021. FTIR and PLS-regression in the evaluation of bioactive amines, total phenolic compounds and antioxidant potential of dark chocolates. Food Chem. 357, 129754. https://doi.org/10.1016/j.foodchem.2021.129754.
Elwers, S., Lieberei, R., 2020. Histological and cytological comparison of seed structures of *Theobroma cacao, T. grandiflorum* and *T. bicolor* relevant to post-harvest processing and product quality. J. Appl. Bot. Food Qual. 248–256. https://doi.org/10.5073/JABFQ.2020.093.031.
Elwers, S., Zambrano, A., Rohsius, C., Lieberei, R., 2010. Histological features of phenolic compounds in fine and bulk cocoa seed (*Theobroma cacao* L.). J. Appl. Bot. Food Qual. 83 (2), 182–188.
Eyamo Evina, V.J., De Taeye, C., Niemenak, N., Youmbi, E., Collin, S., 2016. Influence of acetic and lactic acids on cocoa flavan-3-ol degradation through fermentation-like incubations. LWT - Food Sci. Technol. (Lebensmittel-Wissenschaft -Technol.) 68, 514–522. https://doi.org/10.1016/j.lwt.2015.12.047.
Febrianto, N.A., Zhu, F., 2020. Changes in the composition of methylxanthines, polyphenols, and volatiles and sensory profiles of cocoa beans from the Sul 1 genotype affected by fermentation. J. Agric. Food Chem. 68 (32), 8658–8675. https://doi.org/10.1021/acs.jafc.0c02909.
Galvão, A.C., Souza, P.P., Robazza, W.S., França, C.A.L., 2020. Capacity of solutions involving organic acids in the extraction of the anthocyanins present in jabuticaba skins (*Myrciaria cauliflora*) and red cabbage leaves (*Brassica oleracea*). J. Food Sci. Technol. 57 (11), 3995–4002. https://doi.org/10.1007/s13197-020-04430-5.
García-Plazaola, J.I., Fernández-Marín, B., Duke, S.O., Hernández, A., López-Arbeloa, F., Becerril, J.M., 2015. Autofluorescence: biological functions and technical applications. Plant Sci. 236, 136–145. https://doi.org/10.1016/j.plantsci.2015.03.010.
Gokbayrak, Z.D., Patel, D., Brett, C.L., 2022. Acetate and hypertonic stress stimulate vacuole membrane fission using distinct mechanisms. PLoS One 17 (7), e0271199. https://doi.org/10.1371/journal.pone.0271199.
Gomez, C., Conejero, G., Torregrosa, L., Cheynier, V., Terrier, N., Ageorges, A., 2011. In vivo grapevine anthocyanin transport involves vesicle-mediated trafficking and the contribution of anthoMATE transporters and GST. Plant J. 67 (6), 960–970. https://doi.org/10.1111/j.1365-313X.2011.04648.x.
Hernández-Carrión, M., Hernando, I., Sotelo-Díaz, I., Quintanilla-Carvajal, M.X., Quiles, A., 2015. Use of image analysis to evaluate the effect of high hydrostatic pressure and pasteurization as preservation treatments on the microstructure of red sweet pepper. Innov. Food Sci. Emerg. Technol. 27, 69–78. https://doi.org/10.1016/j.ifset.2014.10.011.
Huang, X.-Y., Wang, C.-K., Zhao, Y.-W., Sun, C.-H., Hu, D.-G., 2021. Mechanisms and regulation of organic acid accumulation in plant vacuoles. Hortic. Res. 8 (1), 227. https://doi.org/10.1038/s41438-021-00702-z.
John, W.A., Kumari, N., Böttcher, N.L., Koffi, K.J., Grimbs, S., Vrancken, G., D'Souza, R. N., Kuhnert, N., Ullrich, M.S., 2016. Aseptic artificial fermentation of cocoa beans can be fashioned to replicate the peptide profile of commercial cocoa bean fermentations. Food Res. Int. 89, 764–772. https://doi.org/10.1016/j.foodres.2016.10.011.
Lima, G.V.S., Gonçalves, C. G. e, Pinto, A.S.O., Silva, E. M. da, Souza, J. N. S. de, Rogez, H., 2024. Impact of post-harvest processing and roasting conditions on the physicochemical properties, phenolic compounds, and antioxidant capacity of cocoa beans from the Brazilian Amazon. LWT 210, 116825. https://doi.org/10.1016/j.lwt.2024.116825.
Mackon, E., Ma, Y., Jeazet Dongho Epse Mackon, G.C., Li, Q., Zhou, Q., Liu, P., 2021. Subcellular localization and vesicular structures of anthocyanin pigmentation by fluorescence imaging of black rice (*Oryza sativa* L.) stigma protoplast. Plants 10 (4), 685. https://doi.org/10.3390/plants10040685.
Markham, K.R., Gould, K.S., Winefield, C.S., Mitchell, K.A., Bloor, S.J., Boase, M.R., 2000. Anthocyanic vacuolar inclusions—Their nature and significance in flower colouration. Phytochemistry 55 (4), 327–336. https://doi.org/10.1016/S0031-9422(00)00246-6.
Martini, M.H., Figueira, A., Lenci, C.G., Tavares, D. de Q., 2008. Polyphenolic cells and their interrelation with cotyledon cells in seven species of *theobroma* (*Sterculiaceae*). Braz. J. Bot. 31, 425–431. https://doi.org/10.1590/S0100-84042008000300006.
Mello Román, J.C., Vázquez Noguera, J.L., Legal-Ayala, H., Pinto-Roa, D.P., Gomez-Guerrero, S., García Torres, M., 2019. Entropy and contrast enhancement of infrared thermal images using the multiscale top-hat transform. Entropy 21 (3). https://doi.org/10.3390/e21030244. Article 3.
Mirjalili, F., Hardeberg, J.Y., 2022. On the quantification of visual texture complexity. J. Imag. 8 (9). https://doi.org/10.3390/jimaging8090248.
Nunes, A.N., Borges, A., Matias, A.A., Bronze, M.R., Oliveira, J., 2022. Alternative extraction and downstream purification processes for anthocyanins. Molecules 27 (2), 368. https://doi.org/10.3390/molecules27020368.
Poobathy, R., Zakaria, R., Murugaiyah, V., Subramaniam, S., 2018. Autofluorescence study and selected cyanidin quantification in the jewel orchids *Anoectochilus* sp. and *Ludisia discolor*. PLoS One 13 (4), e0195642. https://doi.org/10.1371/journal.pone.0195642.
Quevedo, R., Carlos, L.-G., Aguilera, J.M., Cadoche, L., 2002. Description of food surfaces and microstructural changes using fractal image texture analysis. J. Food Eng. 53 (4), 361–371. https://doi.org/10.1016/S0260-8774(01)00177-7.
Ramola, A., Shakya, A.K., Van Pham, D., 2020. Study of statistical methods for texture analysis and their modern evolutions. Eng. Rep. 2 (4), e12149. https://doi.org/10.1002/eng2.12149.
Razgonova, M.P., Zinchenko, Y.N., Kozak, D.K., Kuznetsova, V.A., Zakharenko, A.M., Ercisli, S., Golokhvast, K.S., 2022. Autofluorescence-based investigation of spatial distribution of phenolic compounds in soybeans using confocal laser microscopy and a high-resolution mass spectrometric approach. Molecules 27 (23). https://doi.org/10.3390/molecules27238228.
Re, R., Pellegrini, N., Proteggente, A., Pannala, A., Yang, M., Rice-Evans, C., 1999. Antioxidant activity applying an improved ABTS radical cation decolorization assay. Free Radic. Biol. Med. 26 (9), 1231–1237. https://doi.org/10.1016/S0891-5849(98)00315-3.
Renard, C.M.G.C., Watrelot, A.A., Le Bourvellec, C., 2017. Interactions between polyphenols and polysaccharides: mechanisms and consequences in food processing and digestion. Trends Food Sci. Technol. 60, 43–51. https://doi.org/10.1016/j.tifs.2016.10.022.
Saarniit, K., Lang, H., Kuldjärv, R., Laaksonen, O., Rosenvald, S., 2023. The stability of phenolic compounds in fruit, berry, and vegetable purees based on accelerated shelf-life testing methodology. Foods 12 (9), 1777. https://doi.org/10.3390/foods12091777.
Schneider, C.A., Rasband, W.S., Eliceiri, K.W., 2012. NIH image to ImageJ: 25 years of image analysis. Nat. Methods 9 (7). https://doi.org/10.1038/nmeth.2089.
Singleton, V.L., Rossi, J.A., 1965. Colorimetry of total phenolics with phosphomolybdic-phosphotungstic acid reagents. Am. J. Enol. Vitic. 16 (3), 144–158. https://doi.org/10.5344/ajev.1965.16.3.144.
Stokes, D.J., 2013. 1 - environmental scanning electron microscopy (ESEM): principles and applications to food microstructures. In: Morris, En V.J., Groves, K. (Eds.), Food Microstructures. Woodhead Publishing, pp. 3–26. https://doi.org/10.1533/9780857098894.1.3.
Yoshimizu, Y., Yasuga, H., Iwase, E., 2022. Quantification of visual texture and presentation of intermediate visual texture by spatial mixing. Micromachines 13 (2), 255. https://doi.org/10.3390/mi13020255.
Zhang, H., Wang, L., Deroles, S., Bennett, R., Davies, K., 2006. New insight into the structures and formation of anthocyanic vacuolar inclusions in flower petals. BMC Plant Biol. 6, 29. https://doi.org/10.1186/1471-2229-6-29.
Zhang, Y., Zielinska, M., Vidyarthi, S.K., Zhao, J.-H., Pei, Y.-P., Li, G., Zheng, Z.-A., Wu, M., Gao, Z.-J., Xiao, H.-W., 2020. Pulsed pressure pickling enhances acetic acid transfer, thiosulfinates degradation, color and ultrastructure changes of "Laba" garlic. Innov. Food Sci. Emerg. Technol. 65, 102438. https://doi.org/10.1016/j.ifset.2020.102438.
Zhao, J., Lu, Z., Wang, L., Jin, B., 2020. Plant responses to heat stress: physiology, transcription, noncoding RNAs, and epigenetics. Int. J. Mol. Sci. 22 (1), 117. https://doi.org/10.3390/ijms22010117.